MOLECULAR DYNAMICS SIMULATION OF VAPOR BUBBLE NUCLEATION ON A SOLID SURFACE

Tatsuto Kimura and Shigeo Maruyama

* Department of Mechanical Engineering, The University of Tokyo,
7-3-1 Hongo, Bunkyo-ku, Tokyo 113-8656, Japan

ABSTRACT

Heterogeneous nucleation of vapor bubbles on a solid surface was simulated by the molecular dynamics method. Liquid argon between parallel solid surfaces was gradually expanded, until a stable vapor bubble was nucleated. Argon liquid was represented by Lennard-Jones molecules and each surface was represented by three layers of harmonic molecules with the constant temperature heat bath model using the phantom molecules outside of the three-layers. We used a quite wettable potential parameter on the top surface and changed the wettability on the bottom surface. The wettability was varied by changing the Lennard-Jones potential parameter between argon and solid molecule. With visualizations of the void patterns, molecular-level nucleation dynamics were explored for slowly and rapidly expanding systems. The over-all shape of the vapor bubble or the "contact angle" was measured at the equilibrium condition achieved after the expansion. The waiting period until the nucleation from the rapid expansion was compared with the nucleation rate of classical heterogeneous nucleation theory. The nucleation rate and the critical radius were not much different from the classical theory.

1. INTRODUCTION

Microscopic understandings of phase interfaces have been badly anticipated in theories of traditional macroscopic heat transfer such as condensation coefficient in dropwise condensation, maximum heat transfer in boiling heat transfer, surface tension of a cluster in nucleation theory, and contact angle for the heat transfer of three-phase interface. Furthermore, recent advanced technologies introduced new microscopic problems in heat transfer such as droplet or crystal facet formation in the chemical vapor deposition process and a vapor bubble formation due to the intense laser heating.

In order to understand the molecular level phenomena related to the phase-change heat transfer, we have been performing molecular dynamics simulations of liquid-vapor interface of a liquid droplet [1], contact of liquid droplet on a surface [2], and evaporation and condensation of liquid droplets on solid surface [3]. Furthermore, we have demonstrated the nucleation of vapor bubble on a solid surface using molecular dynamics simulations [4,5]. On the other hand, Kinjo et al. [6] estimated the “waiting time” of the homogeneous nucleation of Lennard-Jones fluid and claimed that the nucleation rate was 8 orders different from the classical theory. In this paper, the time scale of the heterogeneous nucleation of vapor bubble on a solid surface was estimated and compared with the classical heterogeneous nucleation theory by a molecular dynamics simulation complementary to our previous reports [4,5].

We used simple Lennard-Jones molecules for liquid and vapor molecules and further employed the Lennard-Jones function for the interaction potential between fluid and solid molecules. The solid molecules were represented by harmonic molecules with a temperature control using the phantom molecules. By gradually expanding the solid walls to the negative pressure, we could observe the formation of vapor bubble on the surface. Then, the equilibrium shape of the vapor bubble attached to the surface was considered. The measured contact angle was in good agreement with the case of liquid droplet in contact with the surface [2,3]. After determining the pressure level in which the rapid growth of vapor bubble may occur within a manageable period, the liquid volume was rapid expanded

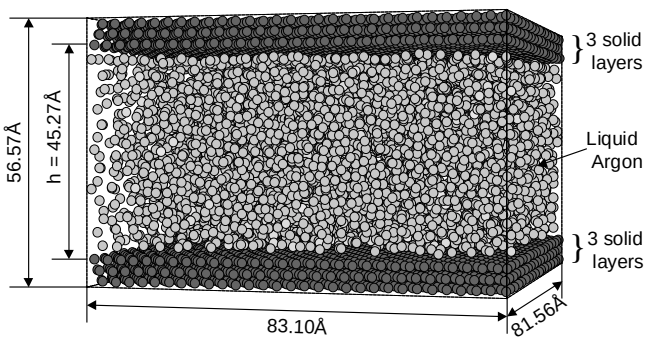

Figure 1 A snapshot of liquid argon between parallel solid surfaces.

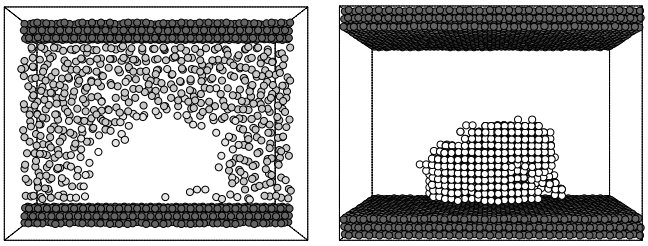

(a) Sliced View (b) Void View

Figure 2 A snapshot of a vapor bubble at 2100 ps for E3.

to this target pressure. Then, the delay of the rapid growth of vapor bubble was measured. By knowing the pressure condition of the successful nucleation, the pressure was rapidly controlled to the target value and the waiting time was estimated. The dynamic behavior of liquid density fluctuations leading to the bubble formation was studied by visualizing the low-density patches of liquid.

2. MOLECULAR DYNAMICS SIMULATION

In order to simulate the heterogeneous nucleation of a vapor bubble on a solid surface, liquid argon consisted of 5488 molecules between parallel solid surfaces was prepared as shown in Figure 1. The potential between argon molecules was represented by the well-known Lennard-Jones (12-6) function as

$$\phi(r) = 4\varepsilon\left\{\left(\frac{\sigma}{r}\right)^{12} - \left(\frac{\sigma}{r}\right)^{6}\right\} \tag{1}$$

where the length scale σ_{AR} = 3.40 Å, energy scale ε_{AR} = 1.67×10^{-21} J, and mass m_{AR} = 6.63×10^{-26} kg. We used the potential cut-off at $3.5\sigma_{AR}$ with the shift of the function for the continuous decay [7]. Even though we could regard the system as Lennard-Jones fluid by the non-dimensional form, here we pretended that it was argon for the sake of physical understanding. The liquid argon was sandwiched by top and bottom solid surfaces, with periodic boundary conditions in four side surfaces.

The solid surface was represented by 3 layers of harmonic molecules (1020 molecules in each layer) in fcc (111) surface. Here, we set as: mass m_S = 3.24×10^{-25} kg, distance of nearest neighbor molecules σ_S = 2.77 Å, the spring constant k = 46.8 N/m, from the physical properties of solid platinum crystal. However, we regarded the solid as a simple insulating material because the effect of free electron and the accurate interaction potential between the metal atom and fluid atom were out of the reach of this paper. We have controlled the temperature of the solid surface by arranging a layer of phantom molecules outside of 3 layers. The phantom molecules modeled the infinitely wide bulk solid kept at a constant temperature T with proper heat conduction characteristics [8,9]. In practice, a solid molecule in the 3rd layer was connected with a phantom molecule with a spring of $2k$ in vertical direction and springs of $0.5k$ in two horizontal directions. Then, a phantom molecule was connected to the fixed frame with a spring of $2k$ and a damper of α = 5.184×10^{-12} kg/s in vertical direction and springs of $3.5k$ and dampers of α in two horizontal directions [4,5]. A phantom molecule was further excited by the random force of Gaussian distribution with the standard deviation

$$\sigma_F = \sqrt{\frac{2\alpha k_B T}{\Delta t}}, \tag{2}$$

where k_B is Boltzmann constant. This technique mimicked the constant temperature heat bath which conducted heat from and to the 3rd layer as if a bulk solid was connected.

Table 1. Calculation Conditions

Label	T_C (K)	ε_{INT}^{BOT} ($\times10^{-21}$J)	$\varepsilon^{*}_{SURF}{}^{BOT}$	θ_{DNS} (deg)	θ_{POT} (deg)
E2	100	0.527	1.86	100.7	101.1
E3	100	0.688	2.42	68.8	66.7
E4	100	0.848	2.99	23.7	19.7
E5	100	1.009	3.56	-	-
E2H	110	0.527	1.86	99.5	102.8
E3H	110	0.688	2.42	61.4	63.0
E4H	110	0.848	2.99	35.0	42.7
E5H	110	1.009	3.56	-	-

The potential between argon and solid molecule was also represented by the Lennard-Jones potential function with various energy scale parameter ε_{INT}. The length scale of the interaction potential σ_{INT} was kept constant as 3.085 Å. In our previous study on the liquid droplet on the surface [2, 3], we have found that the depth of the integrated effective surface potential ε_{SURF} was directly related to the wettability of the surface. Hence, we used a quite wettable potential parameter (ε_{INT} = 1.009×10^{-21} J) on the top surface to prevent from bubble nucleation and changed the wettability on the bottom surface as in Table 1. The solid surface became more wettable from E2 to E5.

The classical momentum equation was integrated by the leap-frog method [10] with the time step of 5 fs. As an initial condition, an argon fcc crystal was placed at the center of the calculation domain of $83.10\times81.56\times56.57$ Å^3 as in Figure 1 (the initial system size was $83.10\times81.56\times58.57$ Å^3 for 110 K). Here, the distance of two solid surfaces h in Figure 1 is used as the reference height of the fluid layer. We used the velocity-scaling temperature control directly to argon molecules for initial 100 ps. Then, switching off the direct temperature control, the system was run for 500 ps with the temperature control from the phantom molecules until the equilibrium argon liquid was achieved. Then, we gradually or rapidly expanded the system volume by moving the top surface at a constant speed. When we measured the equilibrium shape of the vapor bubble, we picked up the time where the vapor bubble was well established as the initial condition and repeated the calculation for 500 ps without the expansion of the volume.

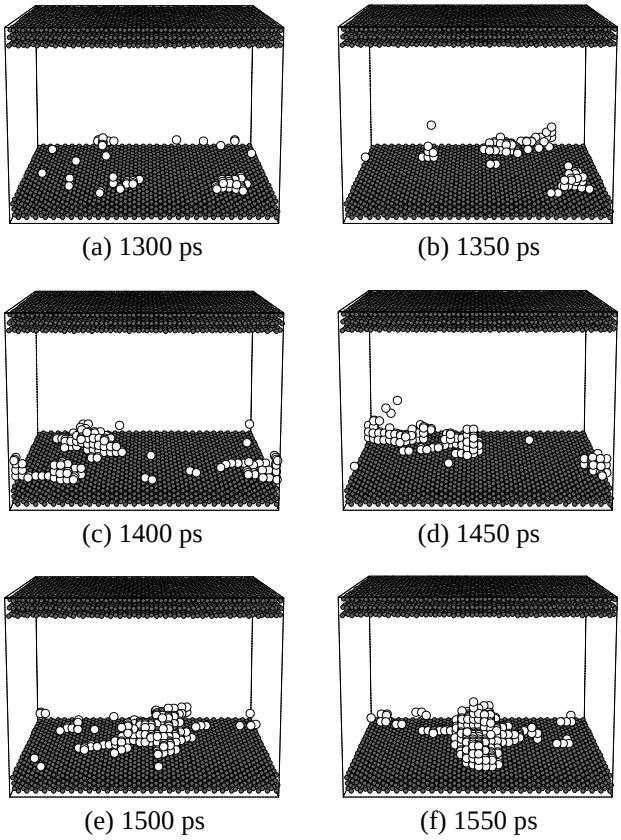

(a) 1300 ps (b) 1350 ps

(c) 1400 ps (d) 1450 ps

(e) 1500 ps (f) 1550 ps

Figure 3 Snapshots of void patterns for E2.

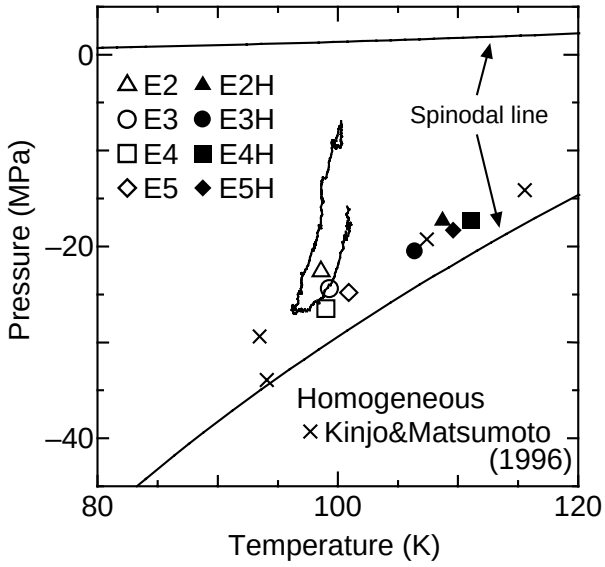

Figure 4 Pressure and temperature variations.

3. SLOW EXPANSION AND EQUILIBRIUM SHAPE OF VAPOR BUBBLE

After the equilibrium of liquid between two solid surfaces at desired temperature was obtained, we slowly expanded the surfaces at 0.5 m/s in the constant temperature condition imposed by the phantom molecules. According to the increase in volume, the decrease of pressure was observed. The pressure variation showed a broad minimum after the expansion and we could observe the formation of vapor bubble in this time range [4,5]. The characteristics of the pressure recovery will be discussed in later section. In order to visualize the density variations leading to the vapor bubble nucleation, we have applied three-dimensional grids of 2Å intervals and visualized the grid as a 'void' when there were no molecules within $1.2\sigma_{AR}$. An example of such a void view representation is shown in Figure 2(b) in comparison with the instantaneous sliced view (Figure 2(a)), which is the well established vapor bubble. Obviously, the assemble of such voids effectively represents the real void or vapor bubble in the liquid. We have traced fluctuations of local density with this instantaneous void view.

Figure 3 shows an example of snapshots for the least wettable condition. There appeared patches of liquid where the local density was considerably low. These patches appeared and disappeared randomly in space and time but preferentially near the bottom surface. Finally, one of the patches successfully grew to a stable vapor bubble on the bottom solid surface where the lower wettability helped to sustain the nucleated bubble. It seems that when the void size is as large as 100 voids (related to about the radius of 10 Å), a single stable vapor bubble stayed on the surface.

We compared the nucleation pressure for various surface potential conditions (wettability) in temperature-pressure diagram in Figure 4. With the increase in the surface wettability, the nucleation pressure approached to the spinodal line (the thermodynamic limit of the existence of superheated liquid, calculated by the molecular dynamics method [11]). The result of the homogeneous nucleation simulation [6] is also plotted in the figure. When a very high wettability of the surface was employed, the situation was closer to the homogeneous nucleation as for E4 and E5. With the decrease in the wettability, the nucleation point moved farther from the spinodal line. These trends are very much in good agreement with the macroscopic concept that the less wettable surface helps the nucleation on the surface.

After detecting the stable vapor bubble formed on the surface, we repeated the simulation for 500 ps without the volume expansion in order to observe the equilibrium structure of the vapor bubble. The two-dimensional density distributions shown in Figure 5 are obtained by cylindrical averaging through the center of the bubble. The layered structure of liquid near the surface is clearly observed. On the other hand, except for about two layers near the surface the shape of bubble can be considered to be a part of a sphere. It is observed that the less wettable surface leads to more flattered shape. These features of the vapor bubble are just the reversed image of our previous molecular dynamics simulation of a liquid droplet near the solid surface [2,3]. We have measured the apparent contact angle by the least square fit of a circle to the density contour line of half of liquid density. Since we have discovered that the cosθ was a linear function of the depth of integrated effective surface potential $\varepsilon^*_{SURF} = \varepsilon_{SURF} / \varepsilon_{AR}$ for the liquid droplet on the surface [2,3], we have compared the present result with the same fashion in Figure 6. It is obvious that the contact angle was in good agreement with

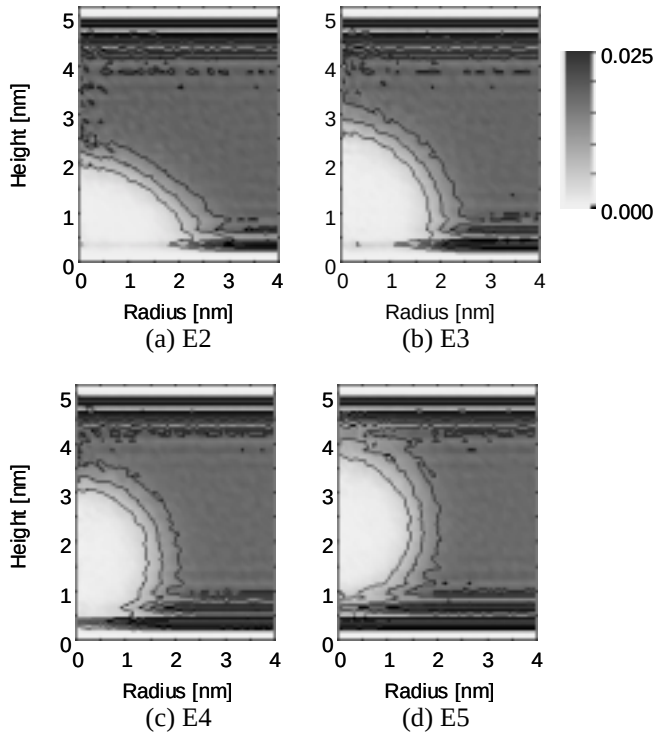

Figure 5 Two-dimensional density distributions.

the case of liquid droplet marked as cross symbols [2,3]. The effect of temperature was small that we could not determine from Figure 6. The slight deviation of the bubble system from the droplet system for larger ε^*_{SURF} is probably due to the employment of Lennard-Jones cut-off for the bubble system.

It is interesting to consider the most wettable surface in Figure 5(d) (E5), in which it is clearly observed that the layered liquid structure completely covered the surface. In Figure 5 it seems that the bubble was just in the middle of two surfaces. However, a slightly smaller bubble in Figure 7 clearly shows that the bubble is still trapped on one of the surfaces [4]. As we monitored the position of the center of bubble, it stayed at almost the same height from the bottom surface, though the ε_{INT} parameters on both surfaces were the same for this condition P5. Even though the effect of the top surface might be concerned because the vertical calculation domain is limited, it is confirmed that the bubble was trapped by the bottom surface. Furthermore, if we extend the definition of the contact angle cosθ to H_c / $R_{1/2}$, the measured point is almost on the line in Figure 6. Here, $R_{1/2}$ is the radius of the fitting circle to the half-density contour, and H_c is the center of the fitting circle. This suggests the possibility of characterizing the liquid-solid contact beyond the apparent contact angle.

4. FORMATION OF VAPOR BUBBLE

In order to investigate the dynamic nucleation process more in detail, the slowly expanding system was not adequate since the pressure condition continuously changed in time. The changes of pressure, temperature, largest void size for slowly expanding system for E3 (Continuous) is shown in Figure 8. In this case the expansion rate was

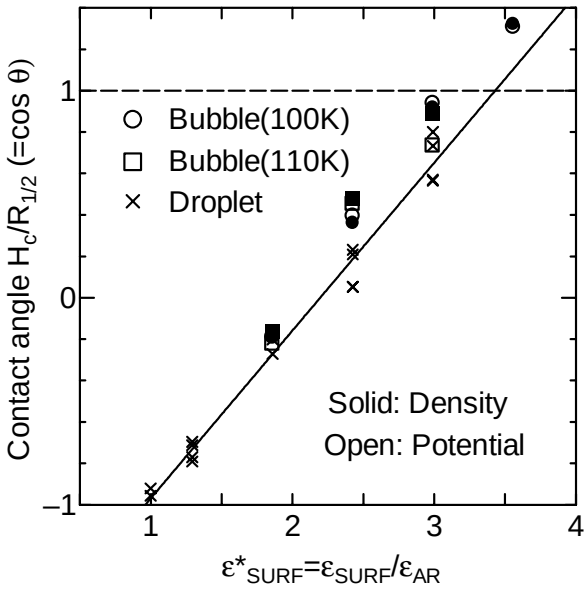

Figure 6 Contact angle correlated with ε^*_{SURF}.

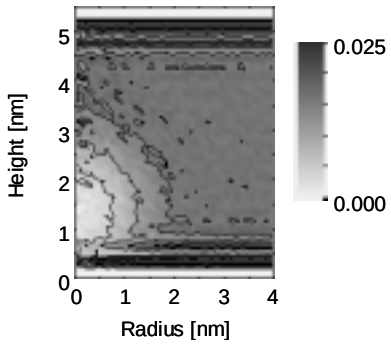

Figure 7 Equilibrium vapor bubble shape for P5 [4].

dh/dt = 5 Å/ns = 0.5 m/s. The rapid increase in void radius at about 1500 ps corresponds to the generation of visible large vapor bubble. The decreasing pressure with expansion began to recover at this time of rapid increase in void radius. This pressure recovery can be attributed to the relaxation of pressure due to the small system size. The isothermal bulk modulus $B_T = -V(\partial p/\partial V)_T$ can be estimated to be 257 MPa from the almost linear decrease of pressure during 500 to 1000 ps (without a large void) due to the expansion. On the other hand, the adiabatic bulk modulus B_{Ad} can be estimated to 471 MPa from our previous report [12]. The sonic speed $\sqrt{(\partial p/\partial \rho)_{Ad}}$ calculated as 602 m/s is in good agreement with the handbook value saturated sonic speed of 696.7m/s at 105K. When the radius of void grew about 20.7Å (Figure 5(b)), the pressure increase is estimated as $\Delta p = -B_T(\Delta V/V)$ = 7.7 MPa. This amount of pressure increase is almost in good agreement with the pressure recovery in Figure 8. This pressure recovery is the intrinsic feature of the small system. If the system size is large enough so that this pressure increase is negligible, principally the same phenomenon as in the macroscopic system is expected. On the other hand, the vapor bubble nucleation in a microscopic channel should have different

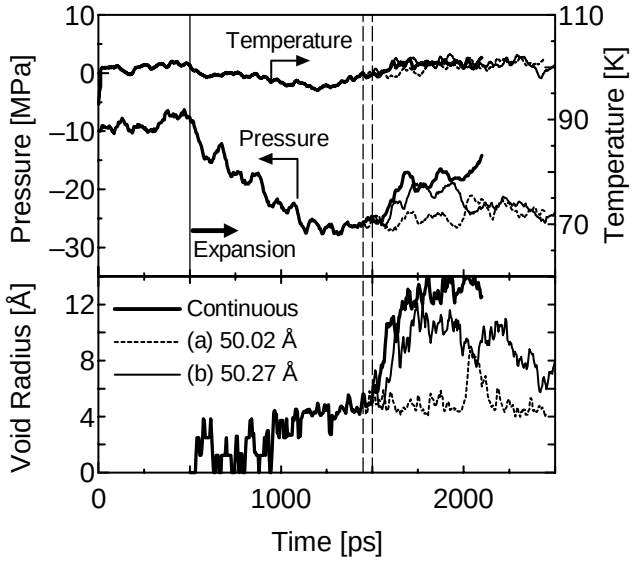

Figure 8 Nucleation process by stopping expansion at certain point.

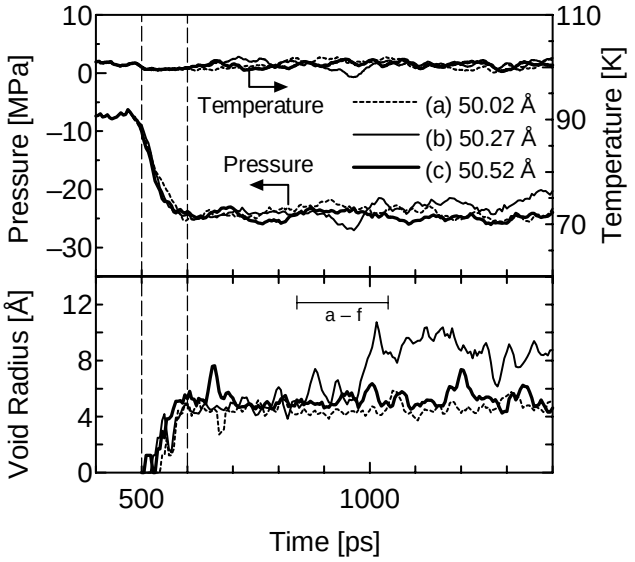

Figure 9 Nucleation process of rapidly expanded system

phenomenon from the larger system that the growth of a single bubble prohibits nucleation of other bubbles by relaxing the supersaturation condition. The existence of the stable vapor in Figure 5 is recognized that the increase of the bubble radius after exceeding the critical radius is suppressed because of the system pressure increase. This system pressure increase can also be understood as the increase of free energy with increase in the bubble radius. In this study, the nucleation process before the sudden and stable increase of vapor bubble is specially considered. The stable increase of the vapor bubble is regarded as the existence of the vapor bubble exceeding the critical size.

In the following simulations, the expansion of the system was stopped after some time, in order to eliminate effects of the gradual increase of volume or the decrease of pressure continued even after the rapid increase of vapor bubble. Figure 8 (a) and (b) show the cases when the expansion was stopped at 1450 ps (h = 50.02 Å) and 1500 ps (50.27 Å), respectively. In the case of Figure 8(b), the rapid growth of vapor bubble was observed a little later than the continuous expansion case. On the other hand, in the case of Figure 8(a), no rapid growth of vapor bubble was observed in about 500 ps even though a considerably large bubble was generated at about 2000 ps. With another stopping time at 1600 ps (50.77 Å), a almost the same rapid growth as for the continuous expansion case was observed (it was not shown in the figure for clarity). Through these trials, it was clear that this expansion amount was almost the threshold value of the observation of rapid growth during the computationally reasonable time scale.

The very rapid expansion of the volume was applied for following simulations. The expansion was done in 100 ps to the expansion amount as in Figure 8. Here, during the rapid expansion, temperature control with the velocity scaling was used in addition to the phantom technique in order to prevent from the too much decrease in temperature. In the case of Figure 9(a), no rapid growth of vapor bubble was observed within 1000 ps as the case in Figure 8 (a). In the case of Figure 9(b), the rapid growth of vapor bubble was observed about 400 ps after the expansion. Since the volume condition is the same between cases in Figure 8(b) and Figure 9(b), it can be recognized that at 1500 ps in Figure 8, the preparation of the rapid growth was already done even though it was not observed in the pressure change or void radius change. On the other hand, no rapid growth of bubble was observed within 1000 ps for Figure 9 (c), even though the pressure should be lower than other conditions.

The change of void patterns for Figure 9(b) case is shown in Figure 10. It can be seen that until the rapid growth of the bubble, generations and decompositions of small voids at random position and time were repeated. At about 1000 ps, a relatively large bubble was suddenly generated and this bubble did grow stably. If the process leading to the rapid growth is stochastic as suggested by these observations, it is impossible to measure the nucleation rate without the numerous simulation trials. However, when a single bubble grows more than the critical size, it suppresses the nucleation of other bubbles in such small system. Then, it is possible to get only one sample of large bubble exceeding the critical radius in each simulation run. With only a few samples of simulation runs, we roughly assumed that the "waiting time" before the rapid growth of a vapor bubble should be the order of 400 ps. The nucleation rate related to this time scale should be $J_{MD} = 1/(A\tau) = 3.7 \times 10^{21}$ cm^{-2}s^{-1}. It can be seen in Figures 8 and 9 than the bubble begin to grow stably when the maximum void radius is more than about 8Å. Then, the critical radius of the bubble should be about 10-15Å (notice the definition of void). This estimation is also dangerous because the growth of a bubble is always accompanied with the relaxation of pressure. Hence, the real critical radius related to the minimum pressure condition might be smaller than this estimation.

For the heterogeneous nucleation of liquid droplet on the smooth surface, the classical theory shows that nucleation rate J is expressed as follows [13-15].

$$J = N^{\frac{2}{3}} S \sqrt{\frac{2\gamma}{\pi m B f}} \exp\left[\frac{-16\pi\gamma^3 f}{3k_B T(\eta p_{sat} - p)^2}\right], \qquad (3)$$

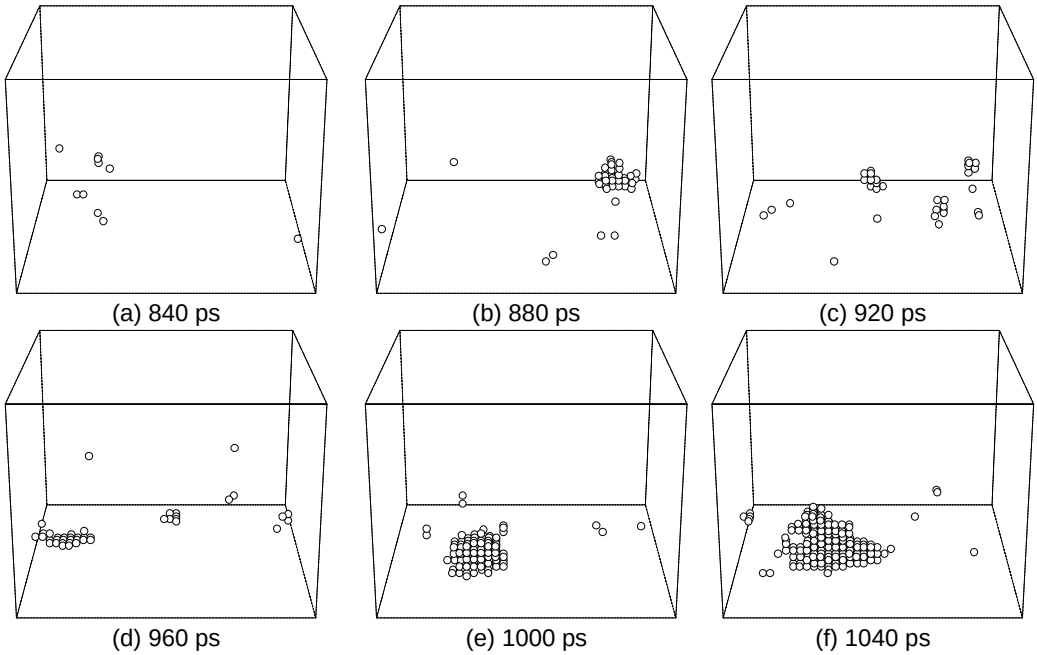

Figure 10 Time history of void pattern (h = 50.27Å)

where

$$S = \frac{1+\cos\theta}{2}, \tag{4}$$

$$f = \frac{1}{4}\left(2+3\cos\theta-\cos^3\theta\right), \tag{5}$$

$$\eta = \exp\frac{\left(p-p_{\mathrm{sat}}\right)}{\rho_l RT}, \tag{6}$$

and the constant B should be unity for cavitations. The critical radius r_e is

$$r_e = \frac{\eta p_{\mathrm{sat}} - p}{2\gamma} \tag{7}$$

The contact angle θ can be estimated from the equilibrium density profile shown in Figure 5. Using the physical properties obtained from the correlation equation for Lennard-Jones fluid [11], the nucleation rate and the critical radius were calculated as $J = 2.0 \times 10^{20}\,\mathrm{cm^{-2}s^{-1}}$ and r_e = 7.9 Å, respectively. These values are not far from the estimation through the simulation, even though the remarkable disagreement for the homegeneous nucleation simulation [6] and classical theory.

This situation is very much similar to the situation for the nucleation of liquid droplet. The molecular dynamics simulation of homogeneous nucleation of liquid droplet by Yasuoka and Matsumoto [16] resulted in 7 orders of differenece from the classical theory, whereas our heterogeneous nucleation of liquid droplet on a solid surface [17] gave a relatively good agreement with the classical theory. The reason is still unclear and we need to further consider the differences in details of simulations and the effect of solid surface. One possible explanation might be that the measured contact angle used in the classical theory made a good link to the simulation result and the theory.

5. CONCLUSIONS

We have successfully demonstrated the nucleation of a 3-dimensional vapor bubble on the solid surface using the molecular dynamics method. The equilibrium shape and the contact angle of the vapor bubble were characterized by the potential parameter just in the same fashion as in the liquid droplet on the solid surface. Furthermore, dynamic behaviors of the low-density patches leading to the bubble nucleation were visualized for several wettability conditions. Through sudden expansion simulations, the "waiting period" before the rapid growth of a vapor bubble was estimated. The order of nucleation rate calculated from this waiting period was roughly in agreement with the classical heterogeneous nucleation theory.

6. NOMENCLEATURE

A:	Area of solid surface
B:	Constant in Eq. (3)
B_{Ad}:	Adiabatic bulk modulus, MPa
B_T:	Isothermal bulk modulus, MPa
H_c:	Center of fitting circle, Å
h:	Distance between two solid surfaces
J:	Nucleation rate, $\mathrm{cm^{-2}s^{-1}}$
k:	Spring constant, N/m
k_B:	Boltzmann constant, J/K
m:	Mass, kg
N:	Number of molecules, Number density
p:	Pressure, MPa
$R_{1/2}$:	Radius of fitting circle, Å
r:	Distance of two molecules, Å
T:	Temperature, K
V:	Volume, $\mathrm{m^3}$
α:	Damping factor, kg/s

Δt: Time step, s
ε: Energy parameter of Lennard-Jones potential, J
ϕ: Potential function
γ: Surface tension, J/m
θ: Contact angle, rad
ρ: Density, kg/m^3
σ: Length parameter of Lennard-Jones potential, Å
σ_F: Standard deviation of exciting force
τ: Waiting period, s

Subscripts
AR: Argon
BOT: Bottom surface
DNS: Density profile
INT: Interaction between argon and solid molecules
i, j: Index of molecule
MD: Molecular dynamics simulation
POT: Potential profile
S: Solid molecule
SAT: Saturated condition
SURF: Integrated for surface
TOP: Top surface

7. REFERENCES

1. S. Maruyama et al., Surface Phenomena of Molecular Clusters by Molecular Dynamics Method, *Thermal Science Engineering*, vol. 2-1, pp. 77-88, 1994.
2. S. Matsumoto et al., A Molecular Dynamics Simulation of a Liquid Droplet on a Solid Surface, *Proc. ASME/JSME Thermal Engineering Joint Conf.*, vol. 2, pp. 557-562, 1995.
3. S. Maruyama et al., Liquid Droplet in Contact with a Solid Surface, *Microscale Thermophysical Engineering*, vol. 2-1, pp. 49-62, 1998.
4. S. Maruyama and T. Kimura, A Molecular Dynamics Simulation of a Bubble Nucleation on Solid Surface, *Proc. ASME/JSME Thermal Engineering Joint Conf.*, AJTE99-6511, 1999.
5. S. Maruyama and T. Kimura, A Molecular Dynamics Simulation of a Bubble Nucleation on Solid Surface, *Int. J. Heat & Technology*, vol. 18-1, pp. 69-74, 2000.
6. T. Kinjo and M. Matsumoto, MD Simulation of the Inception of Vapor Phase in Lennard-Jones Luquids, *Proc. ICHMT Symp*., vol. 1, pp. 215-221, 1996.
7. S. D. Stoddard and J. Ford, *Physical Review A*, vol. **8**, pp. 1504-1512, 1973.
8. J. C. Tully, Dynamics of Gas-Surface Interactions: 3D Generalized Langevin Model Applied to fcc and bcc Surfaces, *J. Chem. Phys.*, vol. 73-4, pp. 1975-1985, 1980.
9. J. Blömer and A. E. Beylich, MD-Simulation of Inelastic Molecular Collisions with Condensed Matter Surfaces, *Proc. 20th Int. Symp. on Rarefied Gas Dynamics*, pp. 392-397, 1997.
10. M. P. Allen and D. J. Tildesley, *Computer Simulation of Liquids*, Oxford University Press, Oxford, 1987.
11. J. J. Nicolas et al., Equation of State for the Lennard-Jones Fluid, *Molecular Physics*, vol. 37-5, pp. 1429-1454, 1979.
12. S. Maruyama et al., A Molecular Dynamics Simulation of Bubble Nucleation on Solid Surface, *Proc. 34th National Heat Transfer Conf. Japan*, pp. 675-676, 1997.
13. M. Blander and J. L. Katz, *AIChE J.*, vol. 21, p. 833, 1975.
14. G. S. Springer, *Advances in Heat Transfer*, Academic Press, vol. 14, pp. 281-346, 1978.
15. R. Cole, *Boiling Phenomena*, McGraw-Hill, I, pp. 71-88, 1979.
16. K. Yasuoka and M. Matsumoto, Molecular Dynamics of Homogeneous Nucleation in the Vapor Phase. I. Lennard-Jones Fluid, *J. Chem. Phys.*, vol. **109**-19, pp. 8451-8462, 1998.
17. T. Kimura and S. Maruyama, Molecular Dynamics Simulation of Nucleation of Liquid Droplet on Solid Surface, *Thermal Science Engineering*, vol. 8-5, 2000 in press.